PHILOSOPHICAL TRANSACTIONS OF THE ROYAL SOCIETY A MATHEMATICAL, PHYSICAL & ENGINEERING SCIENCES

The Ultrastructure of Carbons, Catalytically Active Graphitic Compounds and Zeolitic Catalysts

J. M. Thomas, G. R. Millward and L. A. Bursill

Phil. Trans. R. Soc. Lond. A 1981 **300**, 43-49
doi: 10.1098/rsta.1981.0046

Phil. Trans. R. Soc. Lond. A **300**, 43–49 (1981) [43]
Printed in Great Britain

The ultrastructure of carbons, catalytically active graphitic compounds and zeolitic catalysts

By J. M. Thomas, F.R.S., G. R. Millward and L. A. Bursill†
Department of Physical Chemistry, University of Cambridge, Lensfield Road, Cambridge CB2 1EP, U.K.

[Plates 1–4]

The value of high-resolution electron microscopy as a technique in coal science and technology is illustrated by reference to the study of the onset, on heating, of the crystallinity of relatively unstructured coals and carbonaceous solids; by the detection of changes, upon use, that occur in hydrodesulphurization catalysts; and by the direct imaging of structural features in (*a*) metal catalysts supported on graphitic carbons and (*b*) graphite intercalates of the kind known to be potentially useful in Fischer–Tropsch and related syntheses, which are commercially viable in the conversion of coal to petrols and chemicals.

The technique is also capable of imaging directly the structure of a range of zeolites, including the A, X and Y types, and the ZSM-5 zeolitic catalysts, which figure eminently in the conversion of methanol to petrol. The advantages of high-resolution microscopy, compared with X-ray based methods for the problems peculiar to coal science, are stressed.

1. Introduction

The aim of this paper is to illustrate the advantages of utilizing high-resolution electron microscopy (h.r.e.m.) for (i) the elucidation of the structural details of various categories of carbons and graphites derived from coal (or coal extracts) and (ii) the direct portrayal (at the unit cell level) of the microporosity and structural microheterogeneity of zeolitic solids that are relevant to the production of feedstock chemicals and synthetic fuels such as diesel oil and petrol (gasoline) from coal and its gasified products.

Microporous carbons, including the carbon molecular sieves derived from anthracites (see Walker, this symposium; Walker & Geller 1956; Maggs 1952; Stoeckli 1977) are important as agents for gas purification and separation, and as catalyst supports under acid conditions (as in fuel cells). Their microporosity is probably more reliably assayed by the various techniques that rely on the uptake of gaseous adsorbates rather than by utilizing electron microscopic procedures. This state of affairs follows from the inherent difficulty in interpreting high-resolution structural images of severely disordered or quasi-amorphous materials (see Howie (1980) for a fuller discussion). On the basis of recent work, which shows that theoretically computed, atomically resolved images of amorphous arsenic agree rather poorly with the 'known' structures of such materials (Mallinson *et al.* 1980), it follows that h.r.e.m. is a somewhat unreliable instrument to gauge the ultrastructure of so-called amorphous materials. The situation is, however, very different, when the degree of order is substantial, a fact that becomes apparent later when we discuss the characteristic features revealed by h.r.e.m. of both graphitic supports for metal

† On leave from School of Physics, University of Melbourne, Parkville, Victoria, 3052, Australia.

catalysts and some of the graphitic compounds (intercalates) formed when, for example, ferric chloride is introduced as a guest into the interlamellar spaces of graphite or graphitized coal product.

So far as zeolites are concerned, two facts are of particular importance in the context of new coal chemistry. First, this class of highly porous aluminosilicate (general formula $M_xD_y.Al_{x+2y}Si_{n-(x+2y)}O_{2n}.mH_2O$, where M and D may be monovalent and divalent cations respectively, and n and m are generally large integers) has a wide range of uses in a variety of catalytic processes involving hydrocarbons, ethers and alcohols (see Barrer 1978; Vaughan 1980). The recently developed, high silica 'zeolitic' materials (such as ZSM-5 and ZSM-11; see Meisel, this symposium) are especially important since they serve as catalytic agencies for the facile conversion of methanol to high-octane petrol. They may also be 'tuned' to yield diesel fuels or a range of chemical feedstocks. Their shape-selectivity as well as their remarkable acidity make them exceptional in the degree of control that may be deliberately incorporated into catalysts for given, desired conversions.

2. Types of catalyst and aims of study

We here report four main types of solid studied by h.r.e.m., with procedures that have been discussed previously (Millward & Thomas 1979; Thomas & Jefferson 1978; Millward 1979, 1980; Thomas *et al.* 1979; Bursill 1979; Bursill *et al.* 1980). In essence the technique permits a direct-space (real-space) analysis of local structure. And provided the spherical aberration cofficient of the objective lens of the electron microscope is sufficiently small, the information regarding the structural analysis of these commercially important solids turns out to be reliable and revealing.

(*a*) *Carbon-supported metallic and metal-alloy catalysts*

Finely dispersed particulate Pt-group metals supported on carbon are of commercial importance for a variety of catalytic reactions involving hydrocarbons. The metal catalyst is most commonly dispersed on heat-treated carbon-blacks, channel-blacks, etc., but carbon paper or cloth, activated carbons such as those that are derivable from coal, and the so-called glassy carbons are currently under test. It is well known that processes such as dehydrocyclizations of organic molecules cease to be effective on an otherwise efficient catalyst when the particle size of the supported metal crystallite drops below a certain threshold value. This probably signifies the operation of, *inter alia*, a geometric factor: presumably the organic molecule is not capable of being anchored on the exposed face when the dimensions of the lattice fall below a critical value. One of the principal aims of electron microscopic study is, therefore, to gauge directly the nature, location and size distribution of the metal crystallites, and the degree of crystallinity of the support.

(*b*) *Graphite intercalates*

Many intercalates of graphite, at least on the laboratory scale, exhibit promising degrees of catalytic activity in reactions as diverse as ammonia synthesis (Sudo *et al.* 1969), dimerization of propylene to methylpentenes and of isobutylene to 2,4,4-trimethylpentenes (Hambling & Yeo 1963), alkylation of benzene with propylene (Podall & Foster 1958), hydrodealkylation of alkylaromatics (Ichikawa *et al.* 1973) and the Fischer–Tropsch synthesis (Tamaru *et al.* 1972; Rosynek & Winder 1979). There have been reports that metal chloride, intercalated graphite, when reduced, or when appropriately treated with alkali metal intercalated graphite, yield

particularly efficient catalysts for a variety of reactions, especially the conversion of 'syngas' ($CO + H_2$ mixtures derived from coal gasification with steam) to a range of hydrocarbons and some oxygen-containing products.

(*c*) *Hydrodesulphurization catalysts*

These materials typically consist of molybdenum or tungsten oxides supported on alumina, and deliberately contaminated with cobalt or nickel respectively. At present the precise nature of the cobalt–molybdenum or nickel–tungsten sulphided catalysts, known to be active in the various commercially viable hydrodesulphurization processes of coal and its products, remains obscure.

(*d*) *Zeolitic solids*

Synthetic zeolites of the A, X and Y types (which have progressively increasing Si:Al ratios, starting from the nominal value of unity for the Linde A type zeolite), as well as the rather more structurally complicated and highly siliceous ZSM-5 varieties, are likely to play an increasingly important role in new coal chemical operations. The paper by Meisel (this symposium) illustrates this statement. Up to now, however, owing to the microcrystalline or quasi-crystalline nature of these zeolitic catalysts (i.e. the particle sizes are often less than a few micrometres in maximum linear dimension), X-ray structural methods of identifying and characterizing closely related or newly developed materials have proved inadequate. (This applies equally to the catalytic cracking catalysts, based on the Y zeolite, that have been used over the past few decades.) There is therefore an exigent need for new methods of catalyst characterization (see Lee 1977; Thomas & Lambert 1980). What seems to be particularly desirable at present in catalyst characterization – apart from the ability to monitor changes in a dynamic, *in situ*, sense – are the means of distinguishing whether microcrystalline particles of catalysts are homogeneous (i.e. monophasic) or whether they are biphasic or multiphasic. Moreover, it needs to be known whether, for the highly siliceous, zeolitic aluminosilicates, the Al^{3+} ions are ordered or disordered among the Si^{4+} sublattice.

3. Results and discussion

(*a*) *Carbon-supported metallic and metal-alloy catalysts*

Because of the absence of long-range order and the inherent molecular complexity of coal (see Neavel, this symposium; Pines *et al.*, this symposium), h.r.e.m. yields little or no information relating to structural organization in the parent coal even when the rank of the latter is quite high (Millward 1979; Millward & Jefferson 1978). When, however, certain coal specimens (or coal extracts, the hard brittle material derived from solvent-extracted coal (see Herod *et al.*, this symposium)) are heat-treated, h.r.e.m. reveals directly the gradual emergence of crystallinity. Thus, in figure 1, we see how a specimen of coal extract develops increasing graphitic character as the heat treatment temperature rises from 1300 to 2480 °C, at which temperature the graphitic structure predominates.

So far as identifying minute particles of metallic or alloy crystallites supported on graphitic substrates is concerned, modern high-resolution microscopes can rather easily detect clusters, the diameters of which exceed *ca.* 1 nm or so (figure 2). From such micrographs the particle size distribution of the catalyst, and the preferential location of these crystallites, so important in governing the selectivity and activity of the catalyst itself (see Acres *et al.* 1980), may readily be determined. The morphology of these crystallites is often of crucial importance: raft-shaped

'islands' of supported metal† consisting of no more than a few dozen atoms appear to exhibit distinctly different catalytic activity from that displayed by the more isotropically dispersed material: see Prestridge *et al.* (1977), who studied the size and shape of supported ruthenium–copper and osmium–copper clusters.

With high-resolution microscopes of exceptional performance, it is sometimes possible to identify the nature of the catalyst particle from the resolved atomic planes (see figure 3). Most of the clusters shown in this micrograph are of diameter less than *ca.* 2 nm. With conventional transmission (as distinct from scanning transmission) electron microscopy it is very difficult (both by energy dispersive X-ray analysis and by electron energy loss spectroscopy) to conduct a compositional analysis of catalyst particles of this size.

(*b*) *Graphite intercalates*

As noted above, the intercalates of graphite have been reported to catalyse the synthesis of ammonia, methane, the alkylation of benzene and the dimerization of propylene and isobutylene as well as the Fischer–Tropsch synthesis. Mössbauer and other techniques promise to be important tools for elucidating the mode of action of such catalysts (see Jones 1980), but few techniques afford such detailed, local, structural information as does h.r.e.m. (see Evans & Thomas 1975; Thomas *et al.* 1980).

In figure 4 are to be seen individual '$FeCl_3$ layers' inserted into the interlamellar spaces of the graphite host. Figures 4*a* and 4*b* have been taken under two distinct electron-optical conditions, the former at less than optimal, the latter at the so-called Scherzer defocus value (which corresponds to the most reliable condition for yielding a one–one correspondence between the observed image features and the actual microstructure). Figures 4*c* and 4*d* show, respectively, the computed images (see Jefferson *et al.* 1976) and figure 4*e* the schematic representation of the intercalate itself. At the optimal conditions (figure 4*b*) it is relatively easy to identify both the guest '$FeCl_3$ layer' and the graphitic layers. But in figure 4*a*, recorded under less favourable defocus conditions, the '$FeCl_3$ layer' may again be identified (though rather less readily: note the blurring) whereas the graphitic layers show up in reverse contrast, i.e. the bright horizontal lines correspond to the carbon sheets. (This micrograph illustrates well the danger in relying upon a naïve, intuitive interpretation of electron microscopic images: it is prudent to interpret such micrographs by matching the observed and computer-simulated images under different electron-optical conditions.)

† There could well have been instances when supported metals were wrongly identified as raft-shaped by h.r.e.m. (see Howie (1980) for an instructive discussion).

Description of plate 1

Figure 1. High resolution electron micrographs of coal extract [N.C.B. code 301 (*a*)], heat-treated at (*a*) 1300 °C and (*b*) 2480 °C; see text.

Figure 2. High resolution image of alkali-doped rare-metal catalyst on a graphitized carbon support.

Description of plate 2

Figure 3. Electron micrograph showing two-dimensionally resolved atomic planes in a rare-metal–alkali-metal alloy catalyst on a partially graphitic support.

Figure 4. (*a*, *b*) High-resolution images of a graphite–$FeCl_3$ intercalate taken under different conditions of defocus. As seen from the computed images (*c*, *d*), and the model structure (*e*), reliable information is obtained only from image (*b*), which was taken at the optimum underfocus (94.1 nm). At an underfocus of 130 nm (see (*a*)) the graphitic sheets appear in reversed contrast. Spherical aberration coefficient 2.5 mm.

PHILOSOPHICAL TRANSACTIONS OF THE ROYAL SOCIETY A MATHEMATICAL, PHYSICAL & ENGINEERING SCIENCES

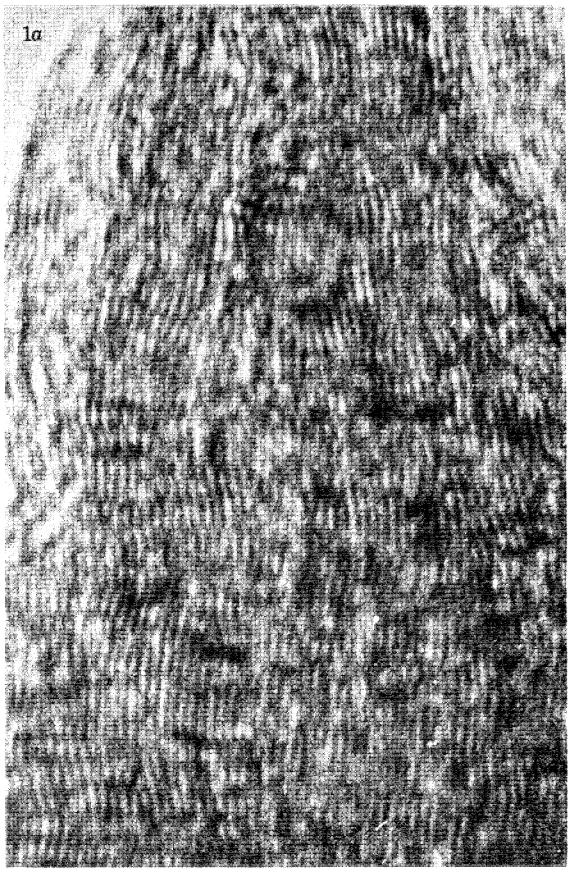

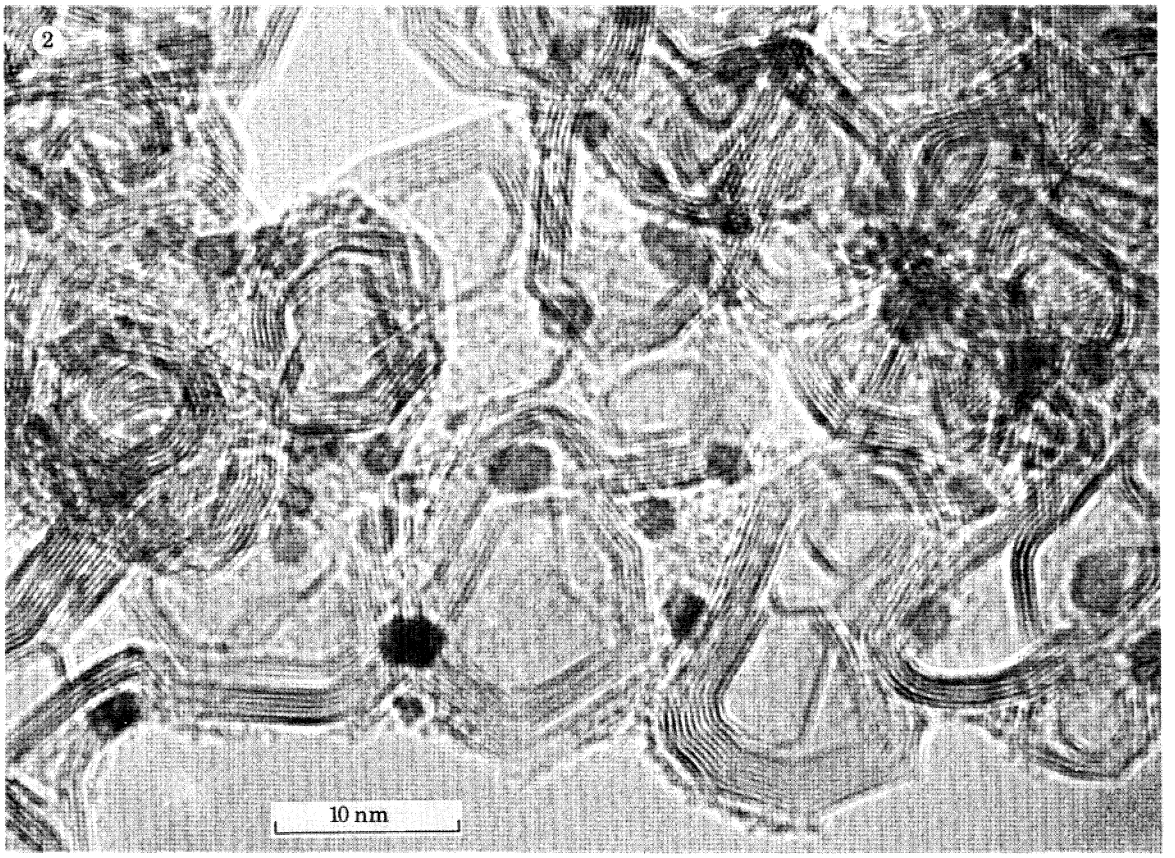

FIGURES 1 AND 2. For description see opposite.

(*Facing p.* 46)

PHILOSOPHICAL TRANSACTIONS OF THE ROYAL SOCIETY A MATHEMATICAL, PHYSICAL & ENGINEERING SCIENCES

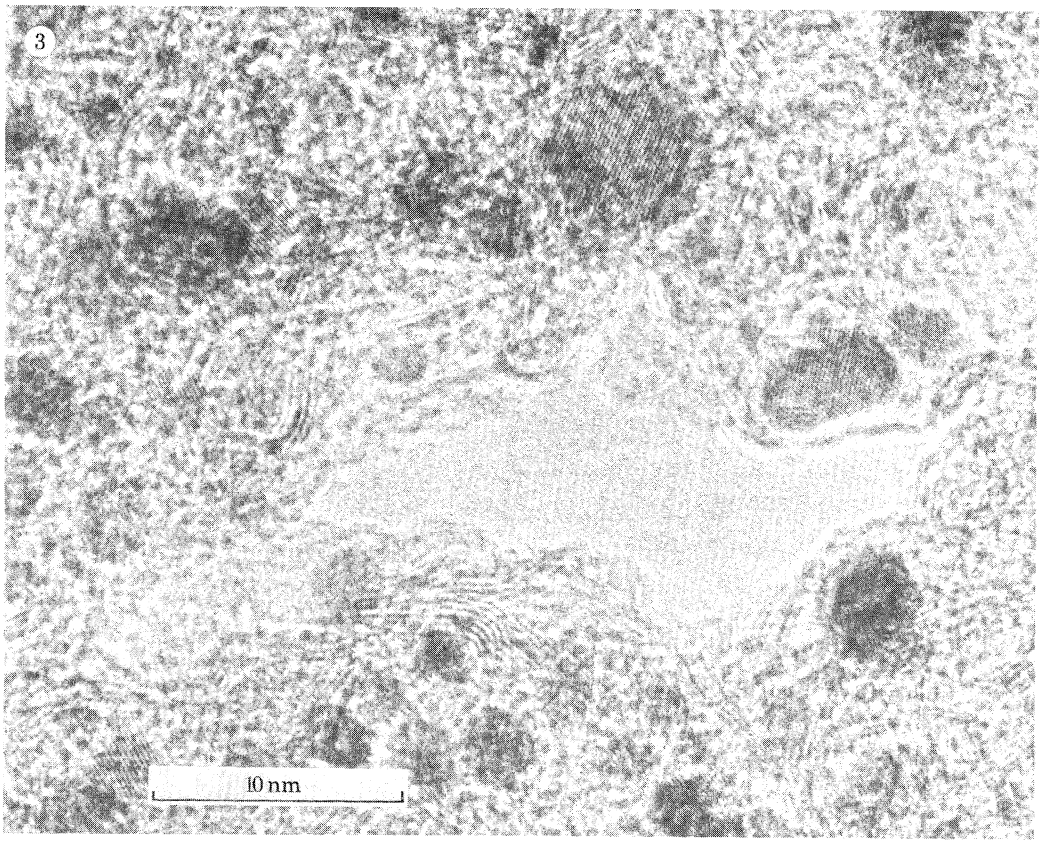

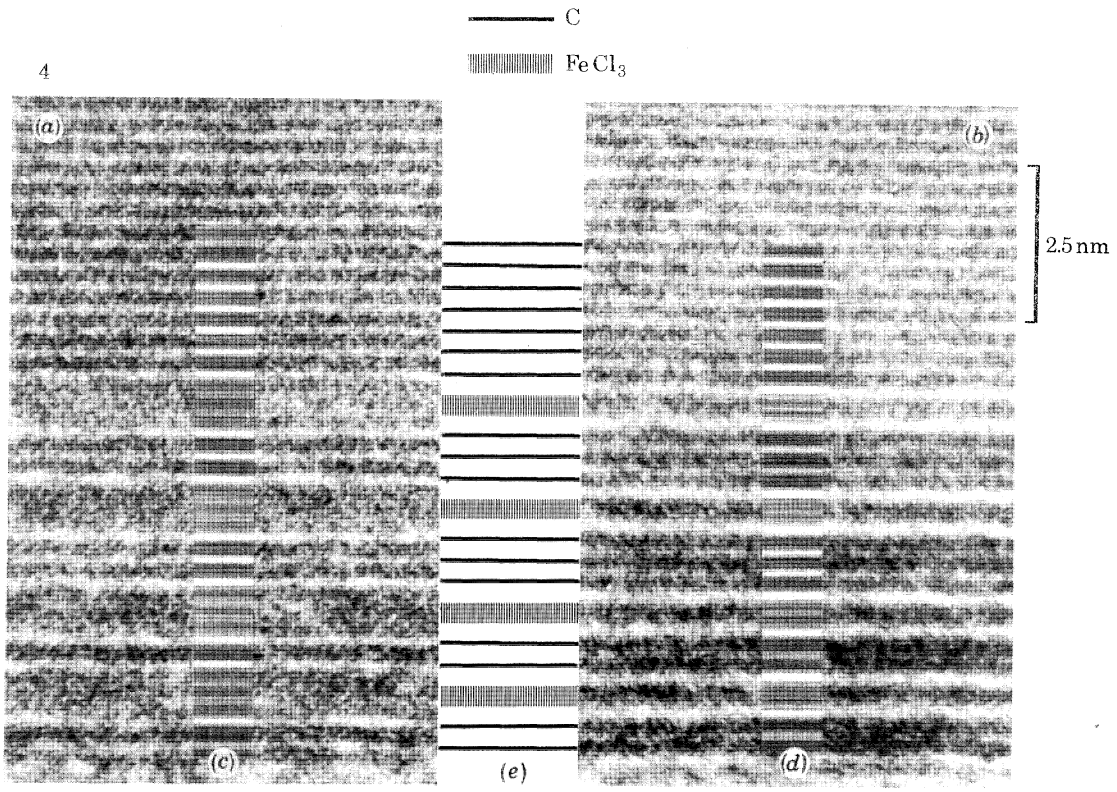

FIGURES 3 AND 4. For description see p. 46.

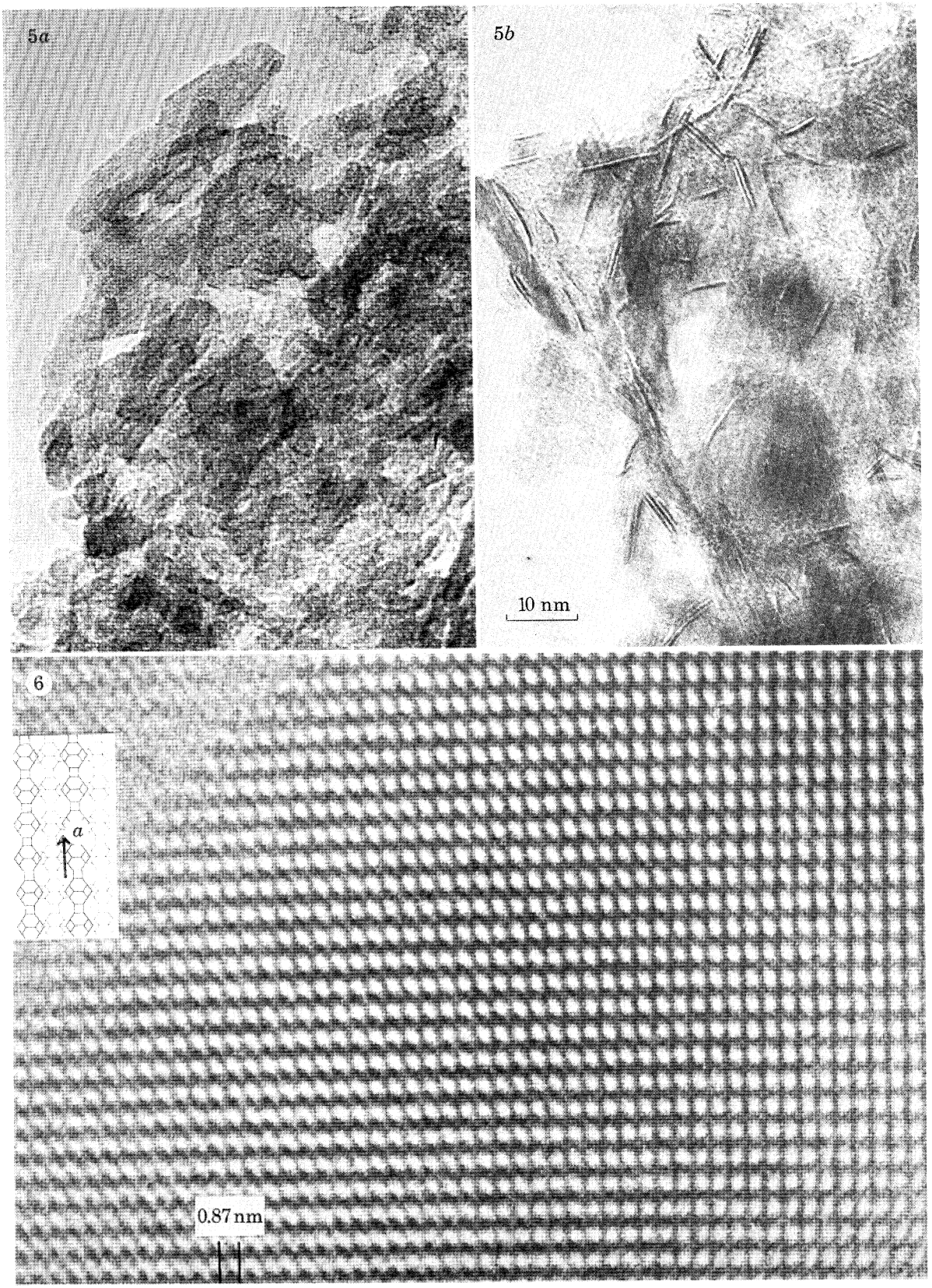

FIGURES 5 AND 6. For description see p. 47.

PHILOSOPHICAL TRANSACTIONS OF THE ROYAL SOCIETY A MATHEMATICAL, PHYSICAL & ENGINEERING SCIENCES

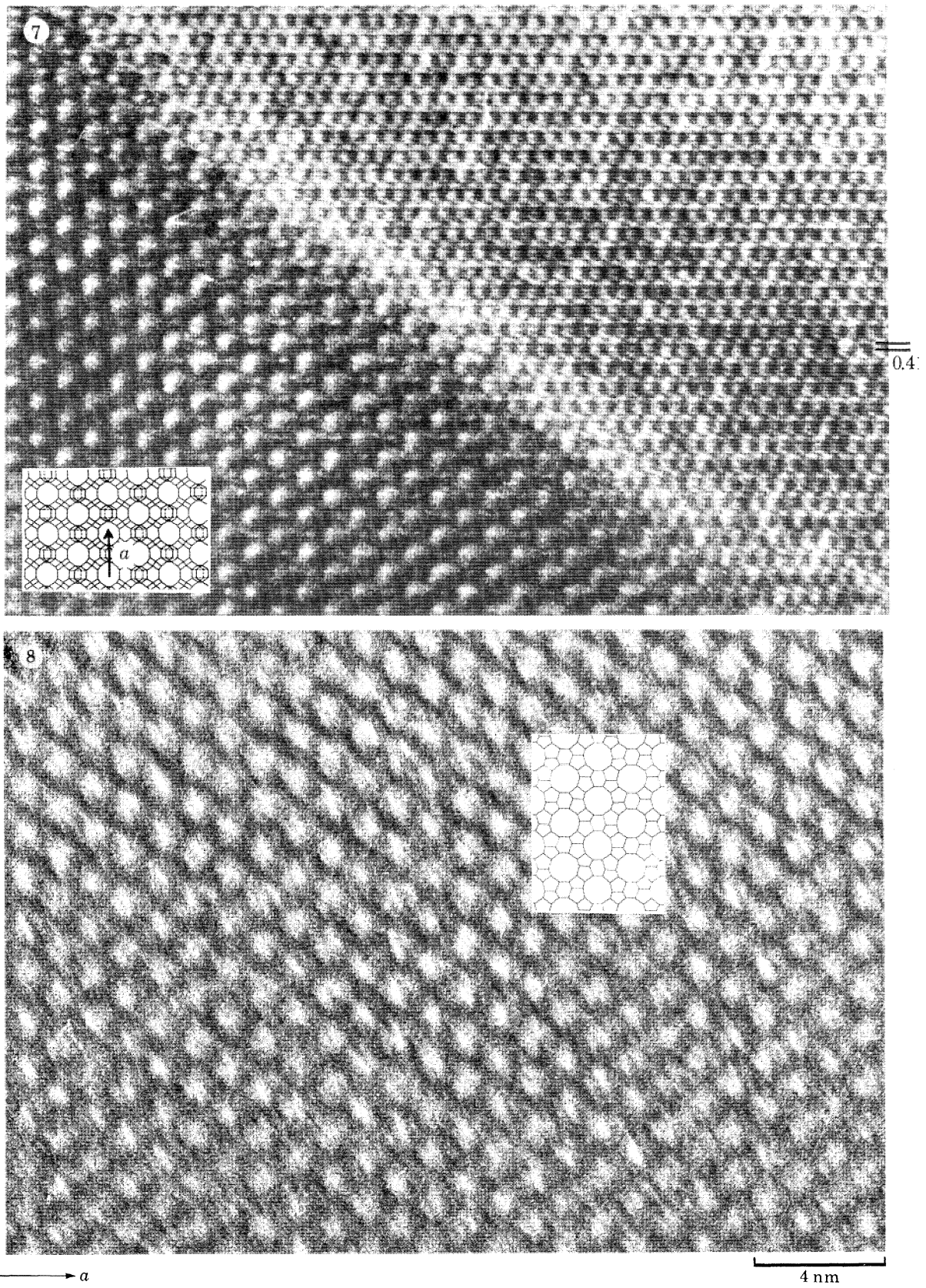

FIGURES 7 AND 8. For description see opposite.

PHILOSOPHICAL TRANSACTIONS OF THE ROYAL SOCIETY A MATHEMATICAL, PHYSICAL & ENGINEERING SCIENCES

(*c*) *Hydrodesulphurization catalysts*

The particular variety of catalyst in this category that we have examined is a commercial preparation of tungsten with nickel supported on γ-alumina pellets. As supplied, the tungsten and nickel are in the form of oxides, the active catalyst being prepared by sulphidation of this precursor. The crystallinity of the γ-alumina in the precursor pellets is evident (figure 5*a*), but h.r.e.m. provides little evidence about the dispersion of the tungsten or nickel oxidic phases. However, the sulphided active form of the catalyst shows clear evidence of well dispersed minute crystallites of WS_2 (figure 5*b*), as identified by the separation of the layers in the crystallites and also by energy analysis of the X-ray emission of localized regions of the specimen. H.r.e.m. is well suited to the detection of the formation of these minute crystallites, which are but a few layers thick, and it would be difficult to obtain comparable information from methods based on X-rays.

(*d*) *Zeolitic solids*

Unlike the microporosity displayed by coals and coal-based carbons, where there is a more or less random spatial dispersion of pores and where the pore diameters cover an immense range (see Walker, this symposium) zeolitic solids possess a well defined intrinsic microporosity, where the pore diameters may be typically 0.5–0.7 nm. The wide range of industrial uses to which zeolitic solids are currently put (see Barrer 1978; Vaughan 1980; Breck 1980) rely principally on this property, especially in their catalytic applications, on the dual advantage of shape-selectivity of the pores and the exceptionally high Brønsted acidity of the solid.

One of the major technical and scientific problems associated with the synthesis, development and use of industrially important zeolitic solids, however, stems from the fact that, almost invariably, only microcrystalline specimens can readily be synthesized and used. (The article by Meisel in this symposium underlines the problem: great effort was required to prepare a single crystal of ZSM-5 large enough to allow X-ray structure determination. (In general, specimens of a newly synthesized zeolite, when crystalline, are too small for X-ray structural analysis, but more often than not they may be severely twinned, only partly crystalline, or multiphasic. Under these circumstances, characterization becomes problematical, and the question of catalyst description and specification looms large. In principle, however, h.r.e.m. can cope with these ostensibly unfavourable circumstances. It possesses the inherent capacity to probe

---

Description of plate 3

Figure 5. Micrographs of a typical W–Ni hydrodesulphurization catalyst: oxidic (*a*) and sulphided (*b*) forms. The minute lamellar crystallites in (*b*) are identified, from the fringe spacing and composition (by X-ray emission analysis), as WS_2.

Figure 6. Structural image, viewed along [011] of a Na-A zeolite. The bright white spots demarcate the intrinsic unit-cell level channels of the structure, which is schematized in the inset.

Description of plate 4

Figure 7. High resolution image of a region of Na-Y zeolite viewed along [110]. In the lower left the observed intensity pattern matches well the expected projected image on the basis of the structure shown, to scale, in the inset. The boundary running across the field of view probably demarcates the interface between two dissimilar phases (see text).

Figure 8. Structural image of ZSM-5 viewed along the *b*-axis. The bright spots demarcate the channels illustrated in the idealized projection (shown in the inset).

PHILOSOPHICAL TRANSACTIONS OF THE ROYAL SOCIETY A MATHEMATICAL, PHYSICAL & ENGINEERING SCIENCES

structure directly (Thomas & Jefferson 1978) in real-space. In practice, however, electron-beam damage may be severe. For zeolites, partly because they are so rich in water but also because they contain some rather readily hydrolysable linkages, beam damage is relatively facile, compared with nephrite jade, or graphitic carbons, for example. We have shown, however (see Bursill *et al.* 1980), that, provided the specimens are extensively outgassed before imaging, and other non-trivial experimental conditions are met, it is possible to obtain rather readily interpretable structural images (at 0.3–0.5 nm resolution) of synthetic A-type zeolite (idealized formula of hydrated form: $Na_{12}(AlO_2)_{12}(SiO_2)_{12}.27\,H_2O$).

Figure 6 shows the structural image, projected along [011] of the Na-A zeolite. From the inset, of the schematized structure of the aluminosilicate (see Olson & Meier 1978), where each vertex represents the location of either a Si^{4+} or Al^{3+} ion, and each connecting line designates an M–O–M bond, with M standing either for Si^{4+} or Al^{3+}, and also from the 0.87 nm repeats, it is clear that the channels running along [011] are clearly imaged. It also follows that the exchangeable cations have become attached to the framework upon dehydration; otherwise the white gaps would be imaged less clearly. Similar images of Na-A (viewed along [001]; see Bursill *et al.* 1980) of Na-X (along [011]), of Na-Y (along [011]) and of ZSM-5 (along [010]) have recently been taken by us.

What is intriguing about the Na-Y image shown in figure 7 is that there appear to be two distinct types of crystal in coherent contact with one another. In the lower left region, as may be judged from the scalar schematic of the projection along [110], the 12-membered rings that form distinct channels in the Y-zeolite stand out clearly. The boundary running from top left to bottom right could demarcate an interface between two different structures. The possibility does, however, exist, though it seems rather unlikely, that a sharp change in thickness occurs on crossing the boundary. Detailed calculations of image variation with thickness may well settle this matter. It is obvious, however, that h.r.e.m. has the power to identify sharp changes in image pattern associated with structural microheterogeneity at little more than the unit cell level.

Figure 8 is the first structural image taken of the remarkable ZSM-5 catalyst. In this particular specimen no obvious microheterogeneities, and no coexistent alumina or other phases, were detected in our preliminary studies of this material. Examination of the new zeolites (described by Taramasso *et al.* 1979), which also appear to be catalytically active ZSM-5 type zeolites containing one of a wide range of substitutional species (such as Ge^{4+} or Co^{2+}) should prove instructive, especially since structural imaging as well as high spatial resolution microanalysis by energy dispersive analysis (Crawford *et al.* 1978) or electron energy loss microanalysis may be carried out.

In addition to the ultra-high resolution imaging, electron diffraction with the use of small areas can be very revealing, since superlattice ordering among the Si^{4+} sublattice (caused by regular insertion of substitutional Al^{3+}), can be detected in and characterized in this way. Recently we have advanced arguments for abandoning the currently accepted space-group for the 4A zeolite. It turns out to be $R\bar{3}$ rather than Fm3c.

We acknowledge with gratitude support from the Science Research Council, the National Coal Board and the University of Melbourne. We are particularly grateful to the following who kindly made available some of the specimens described here: Dr J. Gibson, Dr D. Gavin, Dr R. Schlögl, Dr J. S. Magee and Mr S. Tennison. We also thank Dr D. A. Jefferson and Miss E. A. Lodge for their assistance.

PHILOSOPHICAL TRANSACTIONS OF THE ROYAL SOCIETY A MATHEMATICAL, PHYSICAL & ENGINEERING SCIENCES

References (Thomas *et al.*)

Acres, G. J. K., Bird, A. J., Jenkins, J. W. & King, F. 1980 In *Characterisation of catalysts* (ed. J. M. Thomas & R. M. Lambert), p. 55. London: John Wiley.

Barrer, R. M. 1978 *Zeolites and clay minerals as sorbents and molecular sieves*. Academic Press.

Breck, D. W. 1980 In *Properties and applications of zeolites* (ed. R. P. Townsend), p. 391. London: The Chemical Society.

Bursill, L. A. 1979 *Chemica Scr.* (*Nobel Symp.* no. 47) **14**, 83.

Bursill, L. A., Lodge, E. A. & Thomas, J. M. 1980 *Nature, Lond.* **286**, 111.

Crawford, E. S., Jefferson, D. A., Thomas, J. M. & Bishop, A. C. 1978 *J. chem. Soc. chem. Commun.*, p. 986.

Evans, E. L. & Thomas, J. M. 1975 *J. solid State Chem.* **14**, 99.

Hambling, J. K. & Yeo, A. A. 1963 Br. Pat. no. 932, 342.

Howie, A. 1980 In *Characterisation of catalysts* (ed. J. M. Thomas & R. M. Lambert), p. 89. London: John Wiley.

Ichikawa, M., Tanaka, E. & Tamaru, K. 1973 German Pat. no. 2,209,442.

Jefferson, D. A., Millward, G. R. & Thomas, J. M. 1976 *Acta crystallogr.* A**32**, 823.

Jones, W. 1980 In *Characterisation of catalysts* (ed. J. M. Thomas & R. M. Lambert), p. 114. London: John Wiley.

Lee Lieng-Huang (ed.) 1977 *Characterisation of metal and polymer surfaces*, vol. 1. Academic Press.

Maggs, F. A. 1952 *Nature, Lond.*, **169**, 793.

Mallinson, L. G., Bursill, L. A., Elliott, S. R. & Thomas, J. M. 1980 In *Electron microscopy 1980* (*7th European Congress, Electron Microscopy Foundation*, Leiden) (ed. P. Brederos & G. Boom), vol. 1. (In the press.)

Millward, G. R. 1979 In *coal and modern coal processing: an introduction* (ed. G. J. Pitt & G. R. Millward), p. 87. Academic Press.

Millward, G. R. 1980 *J. Catal.* **64**, 381.

Millward, G. R. & Jefferson, D. A. 1978 In *Chemistry and physics of carbon* (ed. P. L. Walker Jr & P. A. Thrower), vol. 14, p. 1. Marcel Dekker.

Millward, G. R. & Thomas, J. M. 1979 *Carbon* **17**, 1.

Olson, D. H. & Meier, W. M. 1978 *Atlas of zeolite structures*. International Zeolite Association.

Podall, H. & Foster, W. E. 1958 *J. org. Chem.* **23**, 401.

Prestridge, E. B., Via, G. H. & Sinfelt, J. H. 1977 *J. Catal.* **50**, 115.

Rosynek, M. P. & Winder, J. B. 1979 *J. Catal.* **58**, 258.

Stoeckli, H. F. 1977 *J. Colloid Interface Sci.* **79**, 184.

Sudo, M., Ichikawa, M., Soma, M., Ohnishi, T. & Tamaru, K. 1969 *J. phys. Chem.* **73**, 1174.

Tamaru, K., Ohnishi, K., Soma, M., Ichikawa, M. & Sudo, M. 1972 Jap. Pat. no. 7208284.

Taramasso, M., Manara, H., Fattore, V. & Notari, B. 1979 U.K. Pat. no. 2,024,790.

Thomas, J. M. & Jefferson, D. A. 1978 *Endeavour* N.S. **2**, 127.

Thomas, J. M., Jefferson, D. A., Mallinson, L. G., Smith, D. T. & Crawford Davies, E. S. 1979 *Chemica Scr.* (*Nobel Symp.* no. 47) **14**, 167.

Thomas, J. M. & Lambert, R. M. 1980 *Characterisation of catalysts*. London: John Wiley.

Thomas, J. M., Millward, G. R., Schlögl, R. & Boehm, H. P. 1980 *Mater. Res. Bull.* **15**, 671–676.

Vaughan, D. E. W. 1980 In *Properties and applications of zeolites* (ed. R. P. Townsend), p. 294. London: The Chemical Society.

Walker, P. L. Jr & Geller, I. 1956 *Nature, Lond.* **178**, 100.

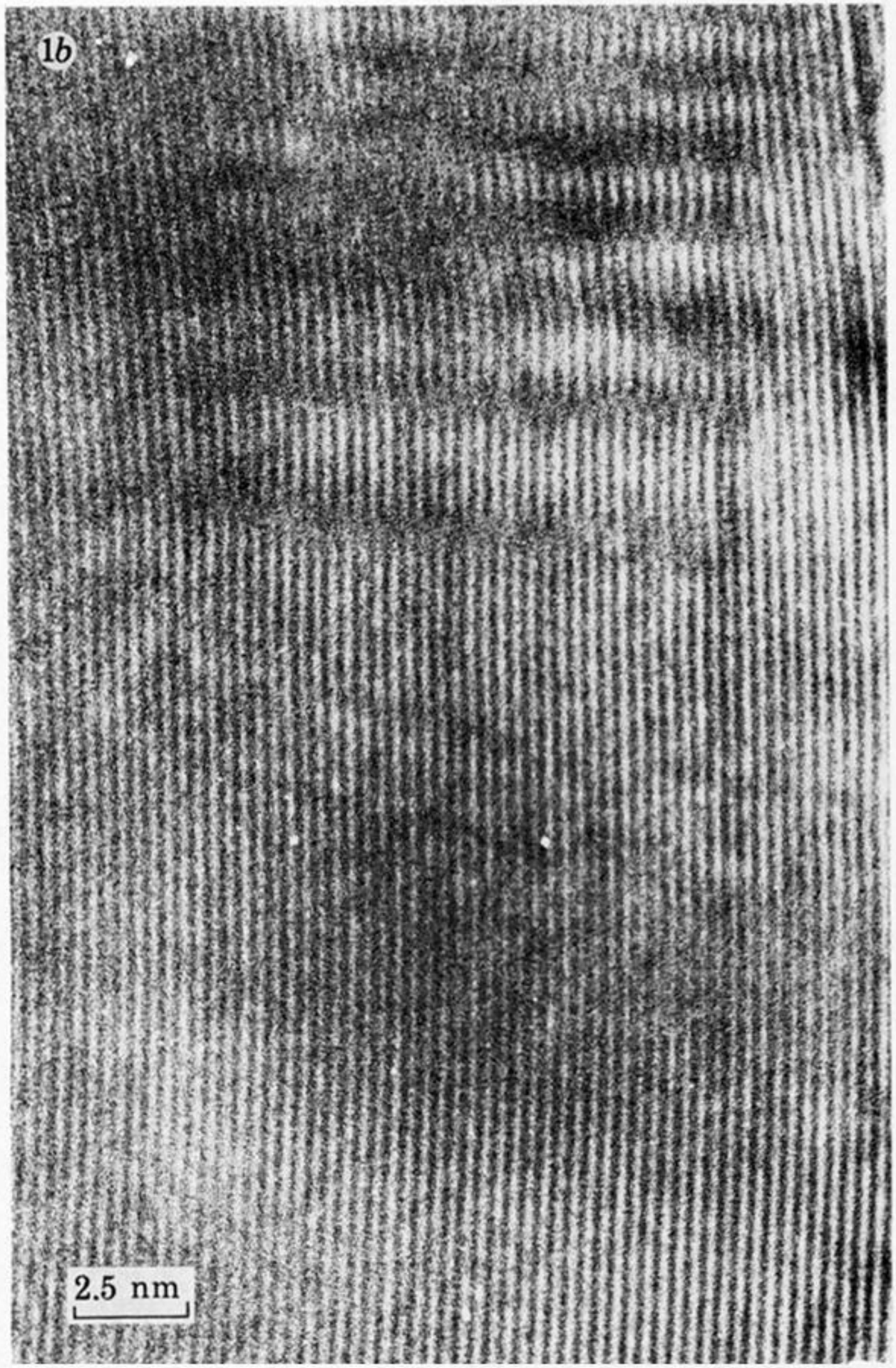

IGURE 1. High resolution electron micrographs of coal extract [N.C.B. code 301 (*a*)], heat-treated at (*a*) 1300 °C and (*b*) 2480 °C; see text.

PHILOSOPHICAL TRANSACTIONS OF THE ROYAL SOCIETY A MATHEMATICAL, PHYSICAL & ENGINEERING SCIENCES

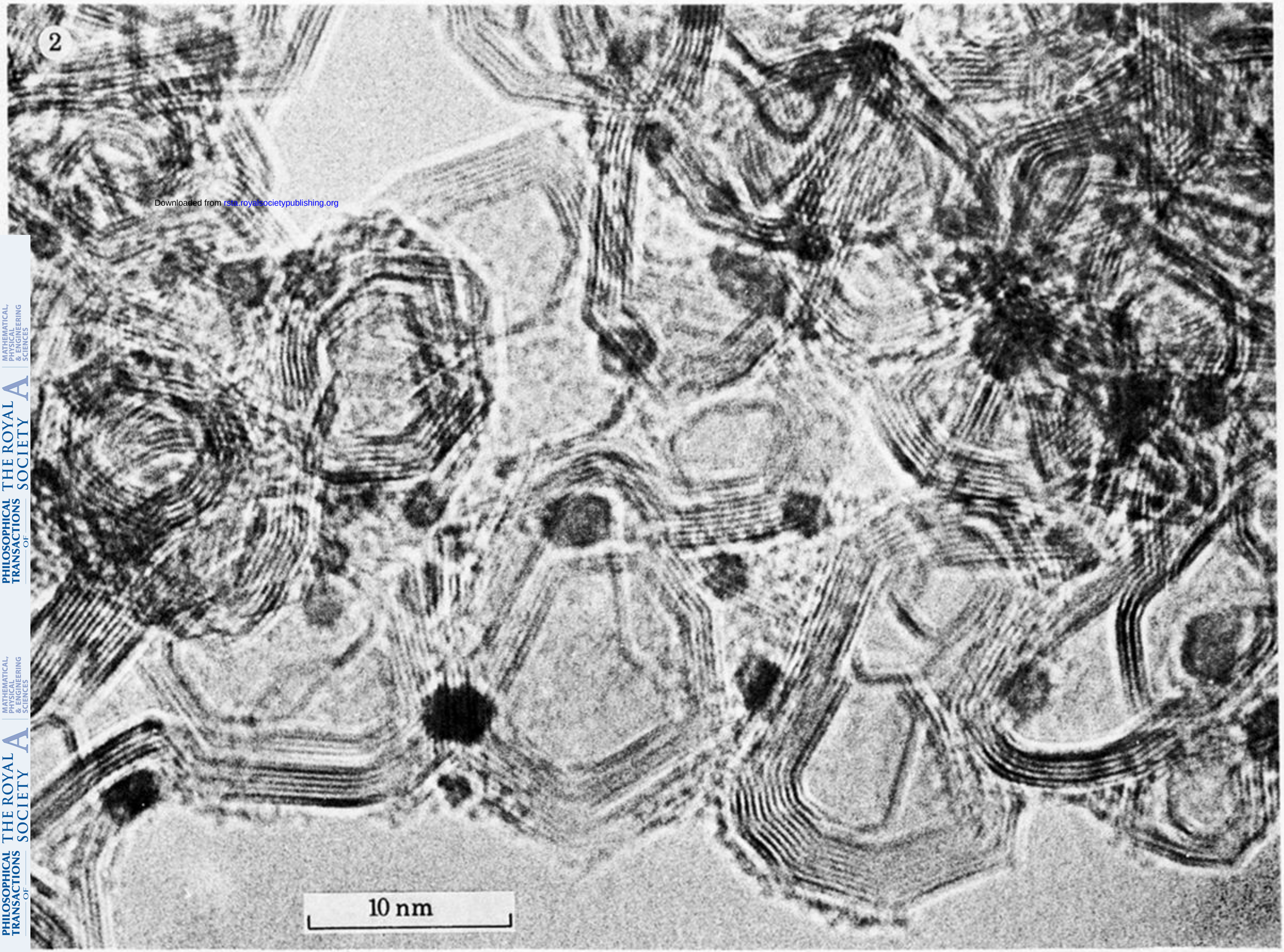

FIGURE 2. High resolution image of alkali-doped rare-metal catalyst on a graphitized carbon support.

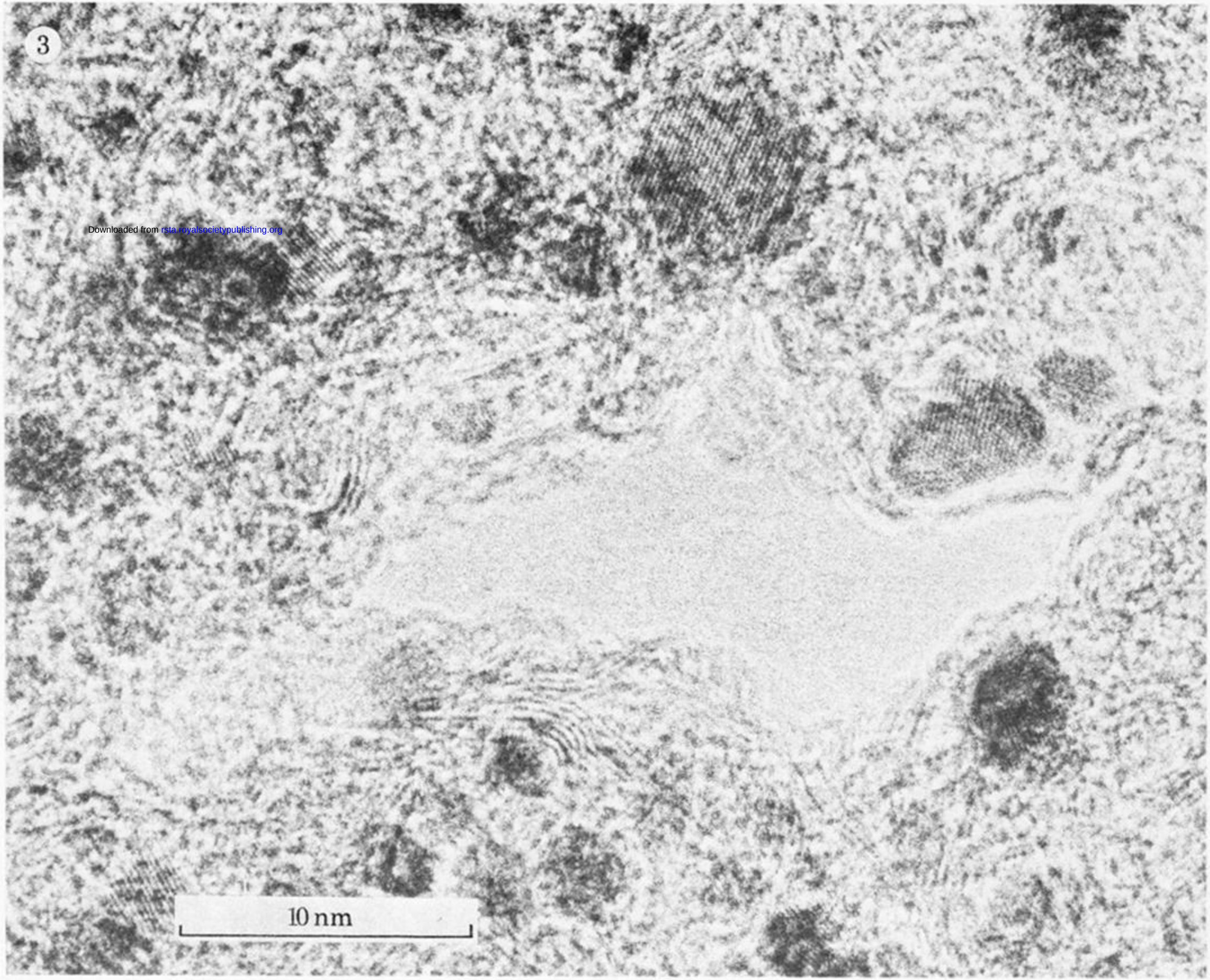

GURE 3. Electron micrograph showing two-dimensionally resolved atomic planes in a rare-metal–alkali-metal alloy catalyst on a partially graphitic support.

PHILOSOPHICAL TRANSACTIONS OF THE ROYAL SOCIETY A MATHEMATICAL, PHYSICAL & ENGINEERING SCIENCES

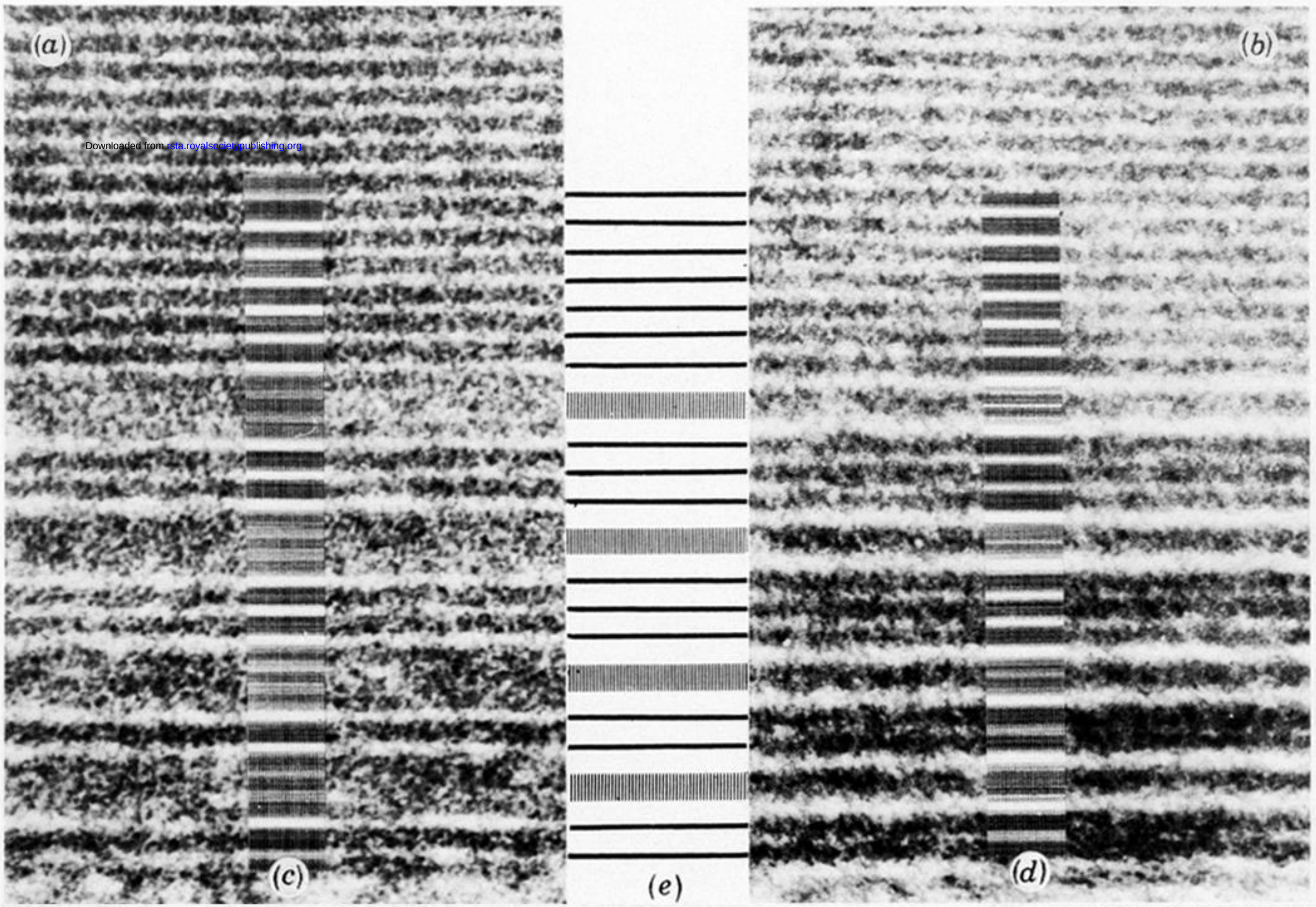

FIGURE 4. (*a*, *b*) High-resolution images of a graphite–$FeCl_3$ intercalate taken under different conditions of defocus. As seen from the computed images (*c*, *d*), and the model structure (*e*), reliable information is obtained only from image (*b*), which was taken at the optimum underfocus (94.1 nm). At an underfocus of 130 nm (see (*a*)) the graphitic sheets appear in reversed contrast. Spherical aberration coefficient 2.5 mm.

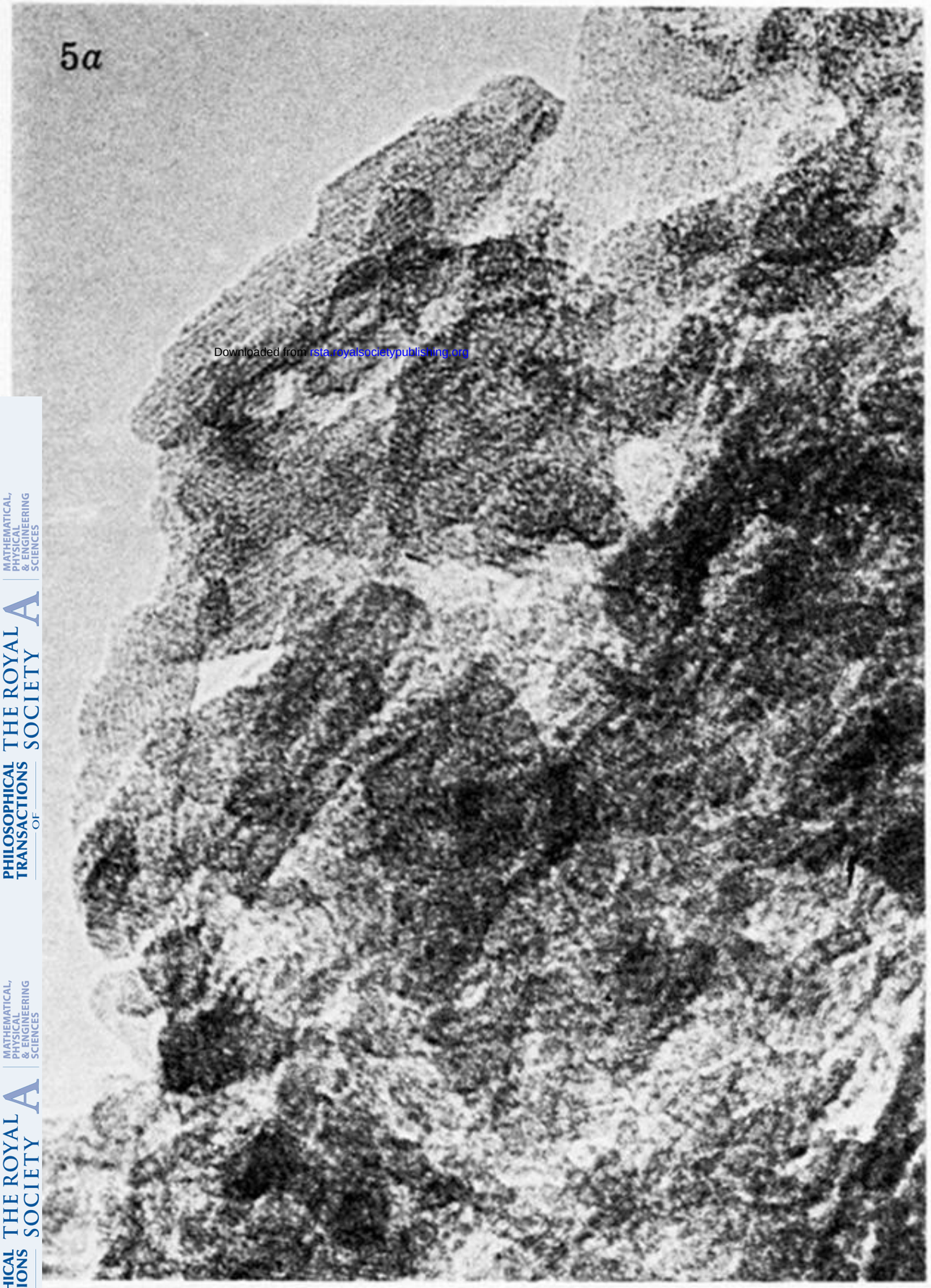

FIGURE 5. Micrographs of a typical W–Ni hydrodesulphurization catalyst: oxidic (*a*) and sulphided (*b*) forms. The minute lamellar crystallites in (*b*) are identified, from the fringe spacing and composition (by X-ray emission analysis), as WS_2.

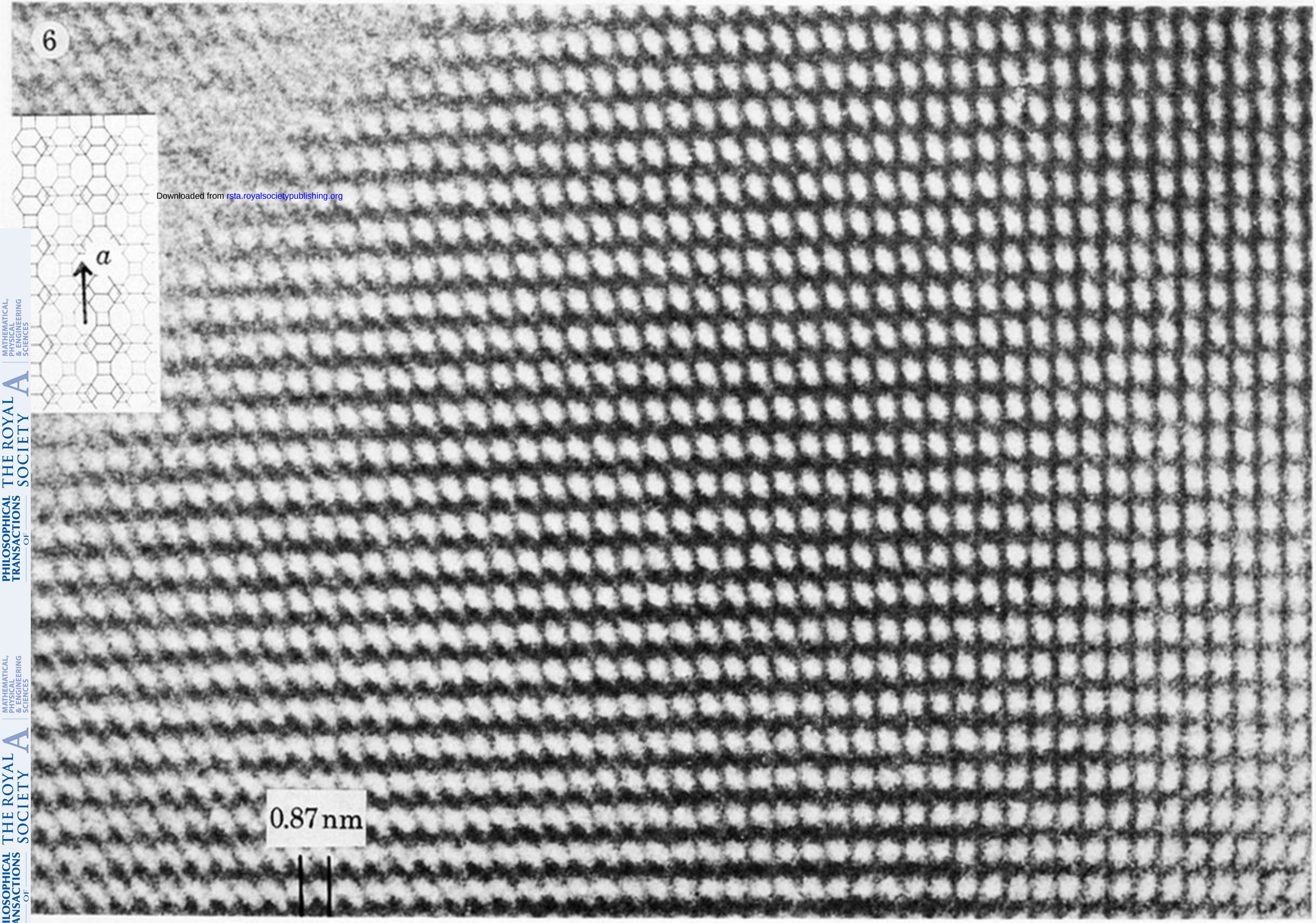

FIGURE 6. Structural image, viewed along [011] of a Na-A zeolite. The bright white spots demarcate the intrinsic unit-cell level channels of the structure, which is schematized in the inset.

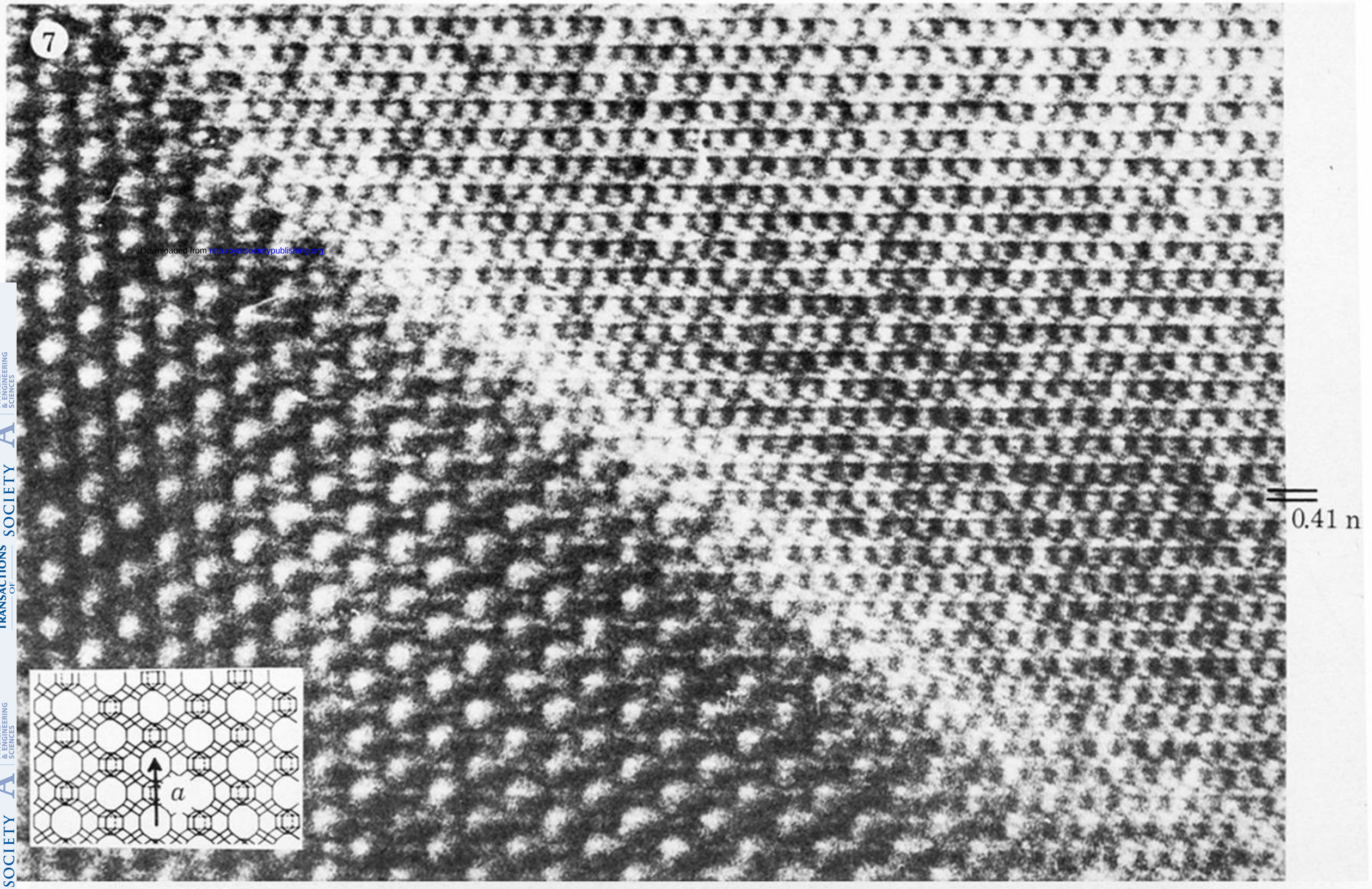

FIGURE 7. High resolution image of a region of Na-Y zeolite viewed along [110]. In the lower left the observed intensity pattern matches well the expected projected image on the basis of the structure shown, to scale, in the inset. The boundary running across the field of view probably demarcates the interface between two dissimilar phases (see text).

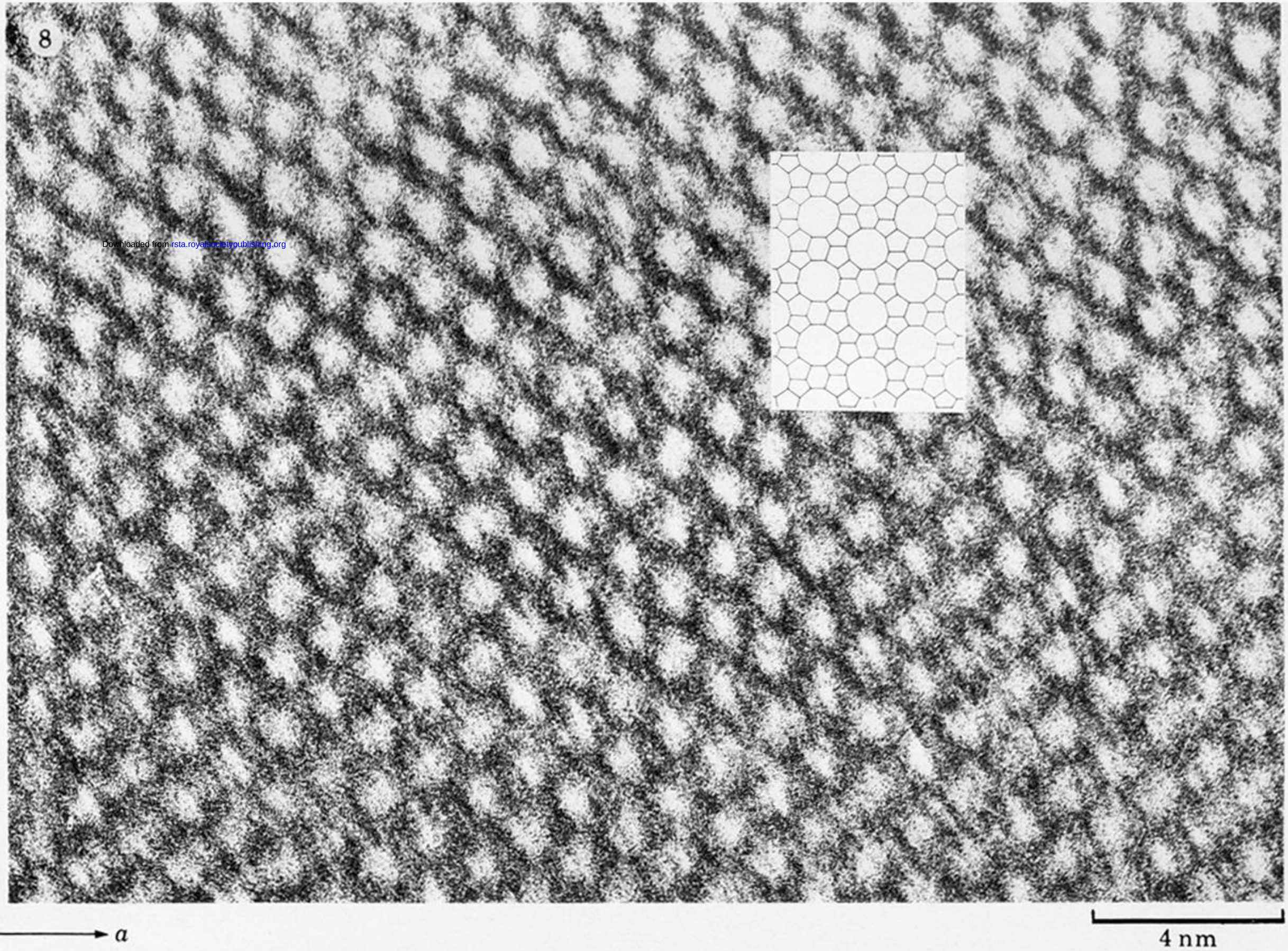

FIGURE 8. Structural image of ZSM-5 viewed along the *b*-axis. The bright spots demarcate the channels illustrated in the idealized projection (shown in the inset).